

# Reduction of magnetic anomaly observations from helicopter surveys at varying elevations

Tadashi Nakatsuka Shigeo Okuma

**Key Words:** magnetic survey, reduction, equivalent source, truncation error, minimum norm, conjugate gradient

## ABSTRACT

Magnetic survey flights by helicopters are usually parallel to the topographic surface, with a nominal clearance, but especially in high-resolution surveys the altitudes at which observations are made may be too variable to be regarded as a smooth surface. We have developed a reduction procedure for such data using the method of equivalent sources, where surrounding sources are included to control edge effects, and data from points distributed randomly in three dimensions are directly modelled. Although the problem is generally underdetermined, the method of conjugate gradients can be used to find a minimum-norm solution. There is freedom to select the harmonic function that relates the magnetic anomaly with the source. When the upward continuation function operator is selected, the equivalent source is the magnetic anomaly itself. If we select as source a distribution of magnetic dipoles in the direction of the ambient magnetic field, we can easily derive reduction-to-pole anomalies by rotating the direction of the magnetic dipoles to vertical.

## INTRODUCTION

Recent developments in aeromagnetic surveying, including improved accuracy of position fixing and navigation, have enabled us to detect more details of subsurface structure. Surveys are accordingly being conducted with narrower line spacings and at lower altitudes. In mountainous regions such as in Japan, helicopter survey flights are required to maintain adequate altitude over rugged terrain, but it is difficult to fly exactly along the planned observation surface.

We are developing an integrated system for helicopter-borne magnetic surveys, from the measuring equipment and data processing to data reduction procedures and interpretation. In this paper we deal with the reduction of magnetic anomalies observed at varying elevations to a consistent surface for further processing or interpretation.

Data processing systems for aeromagnetic surveys in the past were often constructed with the implicit assumption that the observations were acquired on a plane surface, and gridded magnetic anomaly distributions were derived by techniques such as the method of minimum curvature (Briggs, 1974). Where aeromagnetic reconnaissance survey flights are flown at constant barometric altitude, such assumptions may be acceptable. However, for helicopter-borne data acquisition on a draped observation surface, the data processing methodology should be re-examined. Although many authors have discussed techniques for reducing the observed data from one curved surface to another surface,

based upon potential field theory, there is still the problem of how to derive a surface distribution from randomly placed observation points. The observation points should be considered to be randomly distributed in three-dimensional space because the altitude of the helicopter platform may vary from line to line, and survey lines and tie lines may 'cross' with different elevations (strictly speaking, they do not intersect, in three-dimensional space).

In this paper we discuss a data processing scheme for three-dimensionally random observations from a helicopter-borne magnetic survey. The data processing schemes are applied to synthetic model data to demonstrate the advantage of our new scheme, and we also apply them to an actual survey to confirm the validity of our processing method.

## CONTINUATION OF MAGNETIC ANOMALIES BETWEEN ARBITRARY SURFACES

Here we discuss a method of reducing magnetic anomalies observed on one curved surface to another surface. Among the methods for performing such a reduction, the idea of the equivalent source has been discussed by many authors (Dampney, 1969; Nakatsuka, 1981; Hansen and Miyazaki, 1984; Cordell, 1992; etc.). Summarising them, Makino et al. (1993) pointed out that any harmonic function might be the kernel of the integral equation combining the magnetic anomaly distribution with the equivalent-source distribution:

$$F(\mathbf{p}) = \int_S W(\mathbf{p}, \mathbf{s}) E(\mathbf{s}) ds, \quad (1)$$

where  $E(\mathbf{s})$  is the equivalent-source distribution at the point  $\mathbf{s}$  on the infinite (or closed) surface  $S$ ,  $F(\mathbf{p})$  is the magnetic anomaly at the observation point  $\mathbf{p}$  above (or outside)  $S$ , and  $W(\mathbf{p}, \mathbf{s})$  is the harmonic function combining  $F(\mathbf{p})$  with  $E(\mathbf{s})$ . Here all sources are assumed to exist below (or inside) the surface  $S$ . The reduction procedure is as follows. Once we adopt a harmonic function  $W$ , we can estimate the equivalent-source distribution  $E$  as an inverse problem of integral equation (1). Then we can get the magnetic anomaly  $F$  at any position above the surface  $S$  by the forward calculation of the same equation (1). If, as is common, the integration is replaced by numerical integration, equation (1) can be expressed in Cartesian coordinates as

$$F(x, y, z) = \sum W(x, y, z; \xi, \eta, \zeta) E(\xi, \eta, \zeta). \quad (2)$$

The physical meanings of  $W$  and  $E$  have not been mentioned here, as they may be different depending on the form of the harmonic function  $W$ . If we choose  $W$  to be the upward continuation operator,

$$W(x, y, z; \xi, \eta, \zeta) = \frac{-(z - \zeta)}{2\pi \left[ (x - \xi)^2 + (y - \eta)^2 + (z - \zeta)^2 \right]^{3/2}}, \quad (3)$$

then  $E$  is also a magnetic anomaly, on the source surface  $S$ . Makino et al. (1993) called this the "equivalent anomaly", and applied the

Geological Survey of Japan, AIST  
1-1-1 Higashi, Tsukuba, 305-8567, Japan  
Email: tad.nktk@ni.aist.go.jp

Manuscript received July 1, 2005; accepted September 18, 2005.  
Part of this paper was presented at the 111th SEGJ Conference (2004).

method to grid data from a stepped observation surface. As the operator (3) is quite simple and does not become ill-conditioned, the reduction process works quite well.

### EDGE EFFECT AND MINIMUM NORM ANALYSIS

In practice, we deal with magnetic anomaly distributions known only over a limited domain, which gives rise to the problem of edge effect, or truncation error. Equation (1) includes integration over an infinite (or closed) surface, but in actual problems we must restrict the summation in equation (2) to a finite range. The result of this finite-range summation will inevitably have some error, especially in the outer zone.

Nakatsuka (1995) developed a method of introducing surrounding sources in the analysis of magnetisation intensity mapping, and showed that this was able to mitigate edge effects well. Although the inverse problem usually becomes underdetermined because the number of unknown parameters exceeds the number of observation values, asymptotic iteration by the method of conjugate gradients (CG) gives a minimum Euclidean-norm solution. The choice of a minimum-norm solution implies that the result of the analysis is, among probable solutions, the nearest to a reasonable starting model. This is quite desirable in practical applications, because the analysis of potential field data has the essential difficulty that there is no unique solution. (If no other prior information is available, uniformly magnetised terrain is often used as a starting model.)

This idea of obtaining a minimum-norm solution, using surrounding sources to mitigate edge effects, can also be introduced in the data reduction process described in the previous section. Figure 1 is a schematic view of three surfaces with and without surrounding sources. The equivalent-source distribution on the “Surface of eqv. Source” is obtained by inversion of the observational data on the “Obs. Surface”, after which the magnetic anomaly distribution on the “Reduction Surface” can be derived from the equivalent sources.

A synthetic model example is illustrated in Figure 2. Each of the eight panels shows the distribution of either magnetic anomalies or altitudes within a square area of  $6\text{ km} \times 6\text{ km}$ . Panel [B] indicates the altitudes (above sea level) of the observation surface, while [A] is the synthetic total-field magnetic anomaly on that surface. The locations of two source bodies are shown in [D], and their parameters are given in the top right part of the figure. The gently sloping surface also shown in panel [D] is the surface to which magnetic anomalies are to be reduced, and is a smoothed version of the surface in [B]. The theoretical total-field magnetic anomaly on that surface is shown in [C]. Although the magnetic anomaly pattern [A] is similar to [C], there is considerable difference between them.

The data [A] were processed to reduce them to the surface [D]. Panels [G] and [E] are the results from two cases, with and without surrounding sources, respectively. The equivalent-source surface was taken to be 500 m below the reduction surface [D], and source effects were truncated at a horizontal distance of 3 km. The width of the zone of surrounding sources in the calculation of panel [G] was the same as this truncation distance. Even if a much smaller zone width were selected, the result would scarcely differ, as was discussed by Nakatsuka (1995). In this study, a null source was selected as the initial equivalent-source model.

Both reduction results [E] and [G] seem quite similar to the theoretical result [C]. However, there are differences near the bottom left (SW) corner. The differences between [E] and [G] and the ideal result [C] are plotted in [F] and [H], respectively. The effect of ‘source1’ is reconstructed well in both results, because

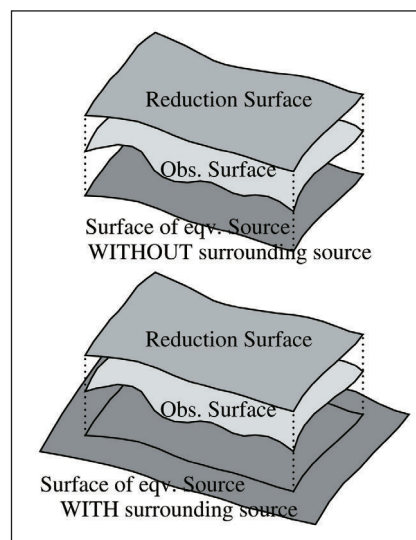


**Fig. 1. Schematic framework of reduction by an equivalent-source technique with or without a surrounding source zone.**

that source is located enough well inside the area of analysis. On the other hand, a relatively large edge effect for ‘source2’ is evident in [E] and [F], where the reduction is performed without surrounding sources, because of the location of the source on the border of the mapped area. The edge effect is very small in the result from the reduction with surrounding sources (panels [G] and [H]).

This example demonstrates that the introduction of surrounding sources into equivalent-source analysis is effective in avoiding edge effect errors.

### EQUIVALENT SOURCE ESTIMATION DIRECT FROM RANDOM POINT DATA

The data processing above is based on gridded data, and the survey data along actual flight lines were interpolated onto a regular grid before the reduction process. We usually use the method of “continuous curvature splines in tension” (CCT method) of Smith and Wessel (1990), which is also implemented in the well-known powerful tool for geophysicists, GMT (Wessel and Smith, 1998).

Gridding programs generally expect input data to be samples of the distribution of a physical quantity on a plane, or at least on a gently sloping surface. In our helicopter surveys, however, adjacent flight paths might be very close to, or even cross, each other, but at different altitudes. Such circumstances, if ignored, might give rise to errors at the gridding stage. To overcome this difficulty, we propose to derive the equivalent-source distribution on some regular surface without grid interpolation, i.e., directly from the recorded survey line data. This will be an underdetermined problem again, because the average line spacing is specified to match the horizontal resolution aimed at in the survey, so the data processing must be detailed enough to represent the required resolution. However, this problem can also be solved using the CG method to find the minimum-norm solution.

To demonstrate the advantage of our proposal, we again begin with a synthetic model. Figure 3 consists of 9 panels [A] – [H] and [L], and each panel covers a  $6\text{ km} \times 6\text{ km}$  square area. The anomalous source parameters are the same as in Figure 2.

We assume 12 lines were flown as in panel [L], and two of them cross each other but are at different altitudes. The numbers written along lines indicate the flight path altitudes, in metres above sea level. There are 1776 observation points in total, at each

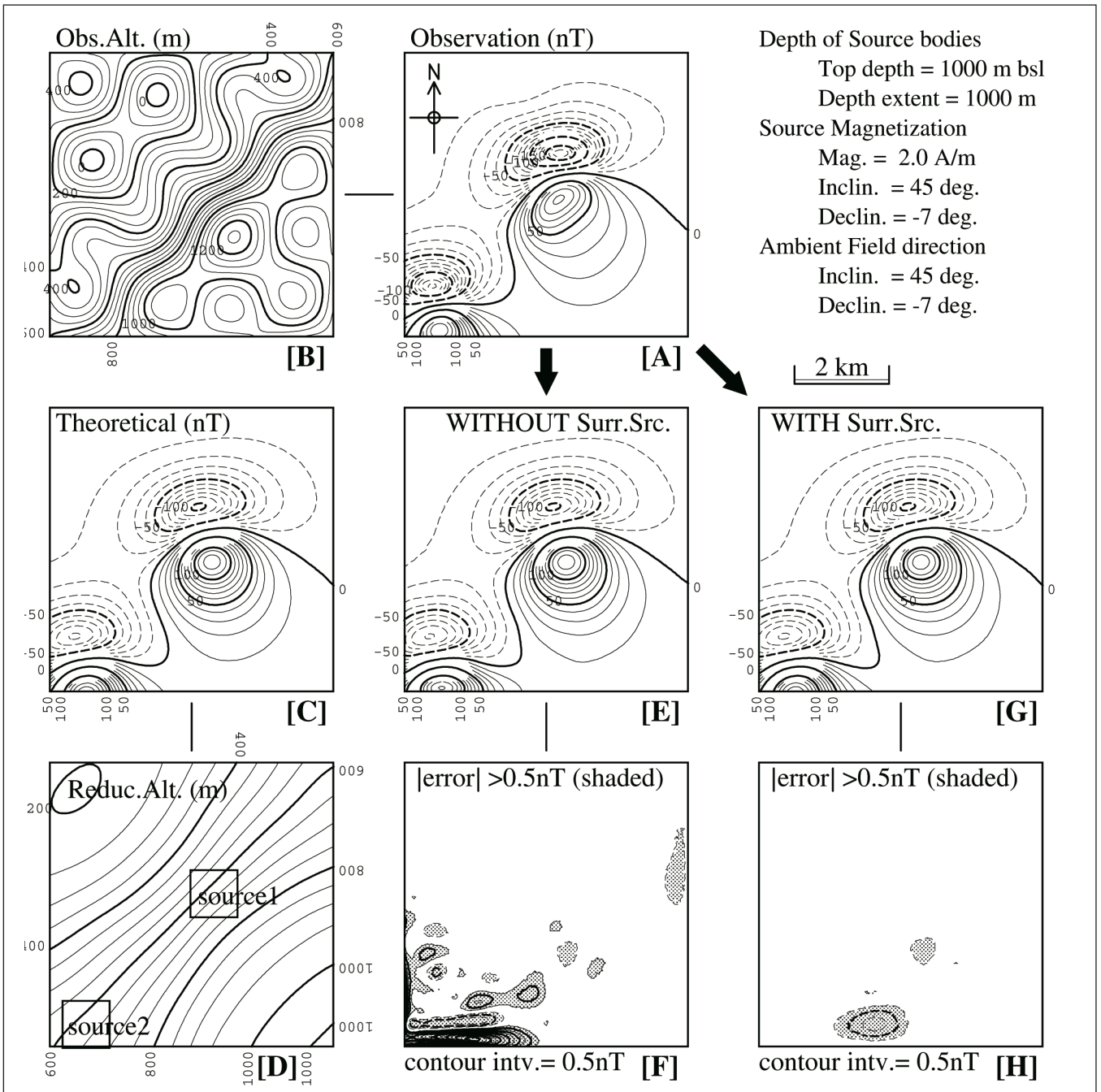


Fig. 2. The effect of a surrounding source zone on reduction, using a synthetic model example. The synthetic total-field magnetic anomaly [A] calculated on the surface [B] was regarded as the observed data. The locations and parameters of anomalous source bodies are shown in [D] and in the top right panel. Two reduction procedures, with and without a surrounding source zone, were applied to derive total-field anomalies on the reduction surface [D], a smoothed version of [B]. The theoretical anomaly [C] on this surface is the ideal result of the reduction process. [G] and [E] are the actual results from the two procedures, and the differences from the ideal [C] are represented in [H] and [F], respectively. [A]–[H] all represent 6 km × 6 km areas. In [B] and [D] altitude contours are at 50 m intervals. In [A], [C], [E], and [G] total-field contours are at intervals of 10nT, and dashed lines show negative values. In [F] and [H] the contour interval is 0.5nT. The edge effects revealed in [F] are reduced by the use of a surrounding source zone, as shown in [H].

of which model total-field magnetic anomalies were calculated theoretically, to be regarded as observed data.

We used the CCT method, after Smith and Wessel (1990), to get magnetic anomaly data on a regular grid, shown in [A]. To determine the topographic (altitude) surface to which the magnetic anomalies in [A] are attributed, we applied the CCT method once more, to the altitudes of the input data, to compute an altitude map, shown in [B]. As these two results are derived independently, there is no valid reason to expect consistency between them. Nevertheless, we regard the magnetic anomaly [A] is having been

observed on the surface [B], as would probably be assumed in conventional data handling. We select the reduction surface [D] (a smoothed version of [B]), as the surface on which a reduced magnetic anomaly distribution is to be derived. The theoretical total-field anomaly on this surface was calculated, and is the ideal result of the reduction process — panel [C].

We applied two reduction methods, one beginning with gridded data [A] and the other working directly from the line data [L]. The results are shown in [E] and [G], respectively. Although both are generally similar to the ideal result [C], differences are noticeable,

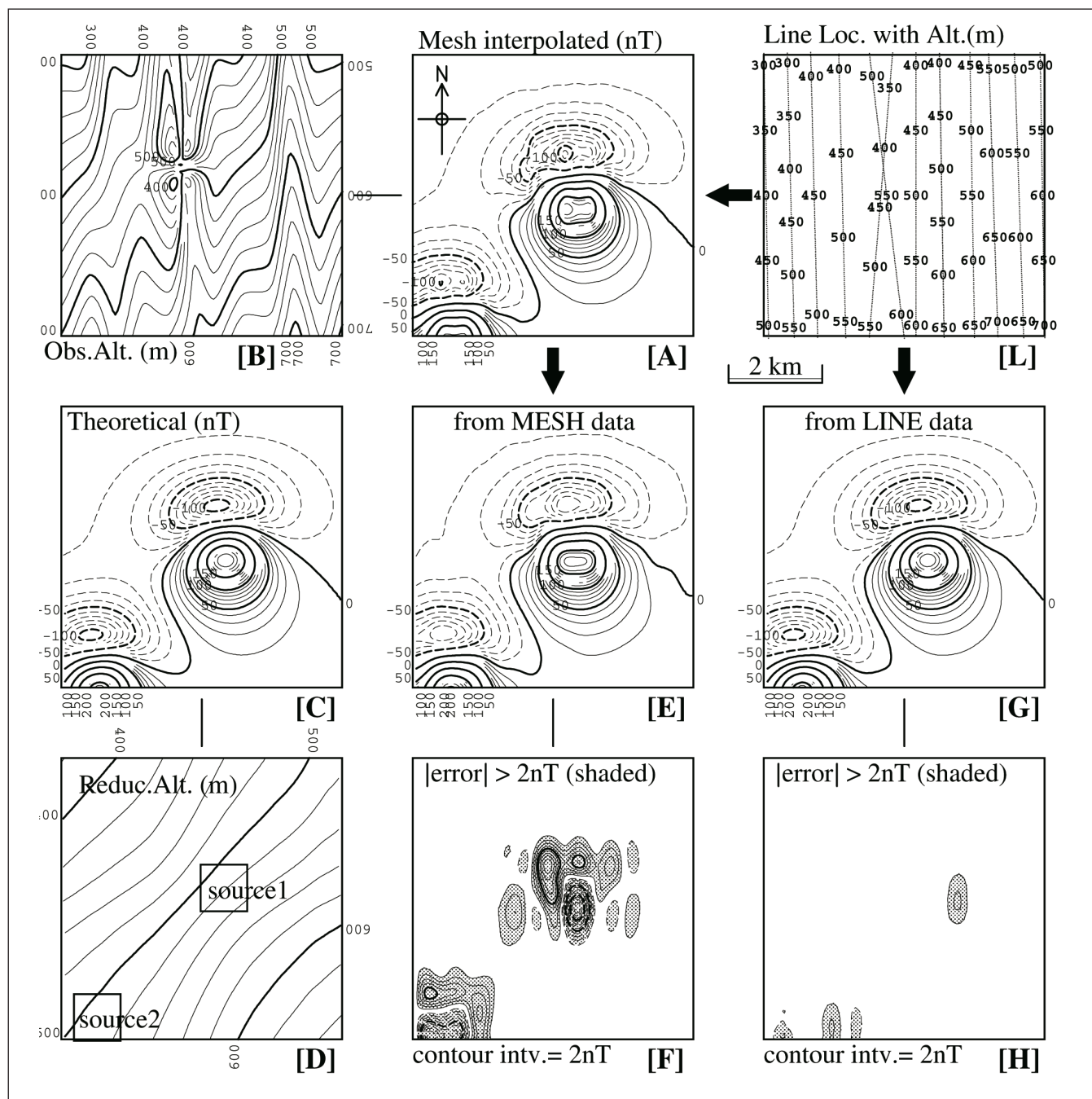


Fig. 3. Comparison of two reduction procedures, one using an intermediate data-gridding step and the other calculating directly from survey line data, applied to the synthetic model example. Synthetic anomalies were calculated along the 12 lines in [L] (at the altitude values shown) using the same anomalous source parameters as in Figure 2. Grid interpolation from this line data gives the total-field anomaly shown in [A] and the altitude surface in [B] using the method of Smith and Wessel (1990). The two data sets, gridded data [A] and survey line data [L], were put into the reduction process to derive total-field anomalies on the reduction surface [D], a smooth version of [B]. The theoretical anomaly [C] on this surface is the ideal result of reduction. Panels [E] and [G] are the actual results from the two processes, and the differences from the ideal [C] are represented in [F] and [H], respectively. In [B] and [D] the altitude contours are at 20 m intervals. Panels [A], [C], [E], and [G] are total-field anomalies with contour intervals of 10nT, where dashed lines show negative values. In [F] and [H] the contour interval is 2nT. Reduction that includes the gridded-data step appears to give less-accurate results, and the direct reduction from line data is preferred.

both in peak values and in distortion of contour lines. To make clear the performance of each method, differences from the theoretical anomaly [C] are presented in [F] and [H], respectively. As these panels show the simple differences (not ratios), there is a tendency for the difference to become larger where the amplitude of the original magnetic anomaly is larger. However, in these panels it is evident that reduction by way of gridded data gives a less-accurate result, especially at shorter wavelengths, and in the zones between survey lines. The method of reduction directly from survey line data is an appropriate, and better, alternative.

### CALCULATION OF REDUCTION-TO-POLE ANOMALIES BY USING EQUIVALENT SOURCES WITH MAGNETISATION DIRECTION

Data from high-resolution helicopter-borne aeromagnetic surveys in mountainous region are reduced to a smooth surface in order to avoid the effect of rapid fluctuations of sensor altitude. If the altitude range is too great, reduction to a horizontal plane might result in a loss of resolution, so generally the data are reduced to a smoothly undulating surface along the topography. As this

surface is not a plane, conventional filtering methods using Fourier techniques are not applicable in principle. Nevertheless, we often want to convert total-field data to reduction-to-pole anomalies, for easier correlation with subsurface structures in the interpretation of magnetic anomalies.

We now investigate the problem of calculating reduction-to-pole anomalies on the undulating surface. We consider a distribution of equivalent sources with specified magnetisation direction properties. If we could obtain an equivalent-source distribution that reproduces the field observation, and whose magnetisation directions coincide with those of actual source bodies, then the reduction-to-pole anomalies can be calculated by rotating the directions of magnetisation, and the ambient magnetic field, to the vertical. As the magnetisation direction of actual source bodies are generally not known, it is usually assumed that the direction of magnetisation is parallel to the ambient magnetic field.

The equivalent-source model we deal with now is a distribution of magnetisation in the direction of the ambient magnetic field, on a specified surface. The formula for calculating total-field magnetic anomalies from such an equivalent-source distribution, when the integration is discretised, results in the summation of magnetic anomalies of point dipoles. This is also given by equation (2) where  $W$  is now

$$W(x, y, z; \xi, \eta, \zeta) = W'(x - \xi, y - \eta, z - \zeta),$$

$$W'(x, y, z) = (V/R^3) [c_x(2x^2 - y^2 - z^2) + c_y(2y^2 - z^2 - x^2) + c_z(2z^2 - x^2 - y^2) + 6c_{xy}xy + 6c_{yz}yz + 6c_{zx}zx], \quad (4)$$

where

$$R = \sqrt{x^2 + y^2 + z^2},$$

$$c_i = e_i p_i \quad [i = x, y, z],$$

$$c_{ij} = (e_i p_j + e_j p_i) / 2 \quad [(i, j) = (x, y), (y, z), (z, x)],$$

$(p_x, p_y, p_z)$  are the direction cosines of the magnetisation vector, and  
 $(e_x, e_y, e_z)$  are the direction cosines of the ambient magnetic field vector.

$V$  can be an arbitrary factor. If we consider  $V$  to be the equivalent volume of each discretised point source, the quantity  $E$  in equation (2) becomes magnetisation (e.g., in A/m). In actual calculation, the inverse problem of equation (2) is solved first using the CG method, with the direction cosines given their observed values. Once the equivalent-source distribution  $E$  has been found, the reduction-to-pole anomalies are given by the forward calculation of equation (2), with the two directions set vertical (i.e.,  $p_x = p_y = e_x = e_y = 0$ , and  $p_z = e_z = 1$ ).

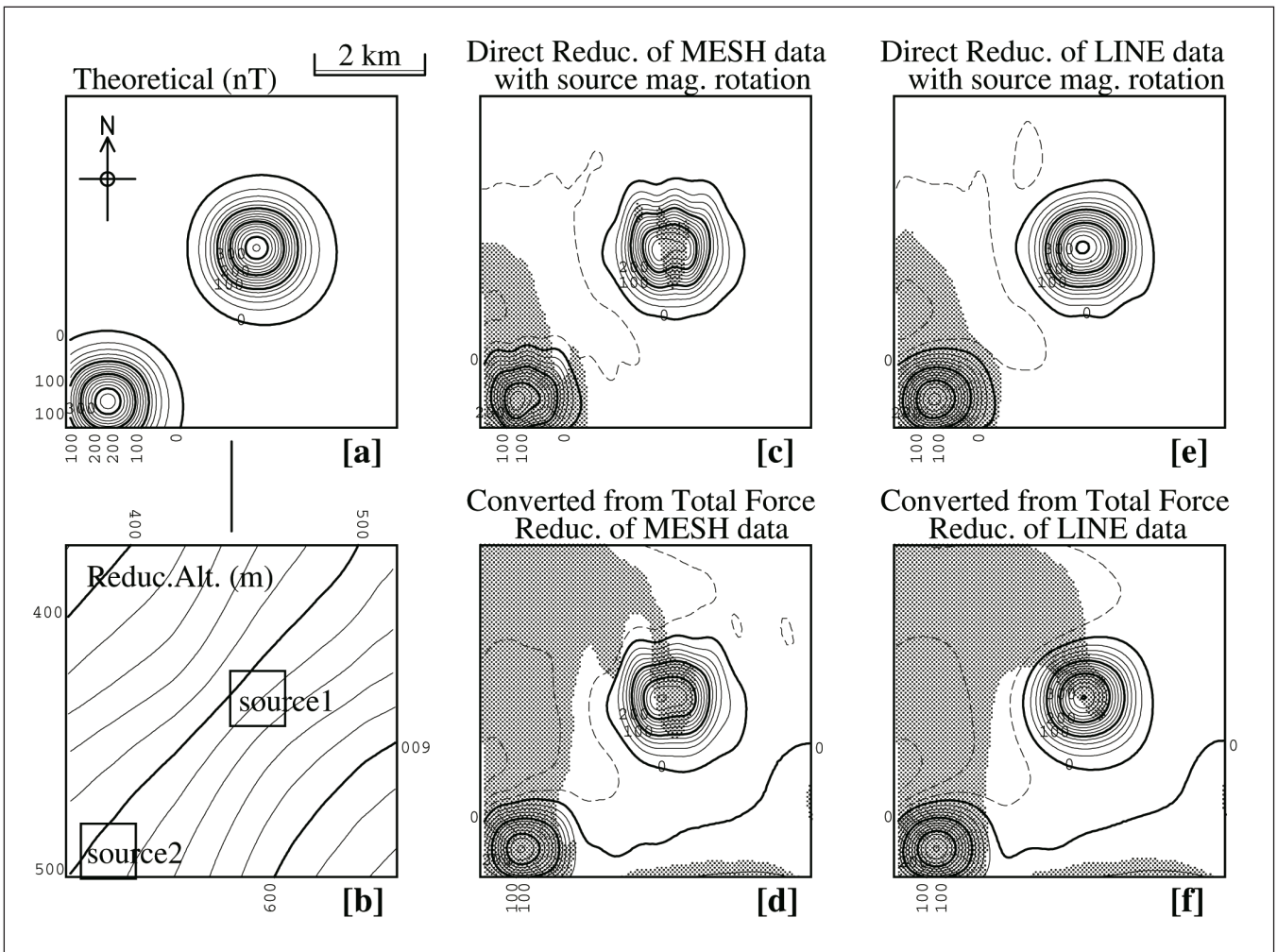


Fig. 4. Calculation of reduction-to-pole anomalies using the synthetic model of Figure 3. There are four results [c]–[f], all of which are a reduction-to-pole anomaly calculated on the reduction surface [b]. The ideal result is the theoretical one [a]. The results [c] (from gridded data) and [e] (from survey line data) are derived by the method of rotating equivalent-source magnetisation, while [d] and [f] are from the conventional Fourier series calculation (applied to the data of Figure 3 [E] and Figure 3 [G], respectively). Panels [c]–[f] have contours at 20nT intervals, and the areas in which differences with [a] exceed 20nT are shaded.

Figure 4 illustrates the results of this method applied to the same model example as in Figure 3. Here the direction parameters of  $45^\circ\text{N}$  inclination and  $7^\circ\text{W}$  declination for both magnetisation and ambient magnetic field were used ( $p_x = e_x = 0.702$ ,  $p_y = e_y = -0.086$ ,  $p_z = e_z = 0.707$ ). There are six panels [a] – [f] in Figure 4. Panel [b], which is the same as Figure 3 [D], shows the shape of the reduction surface and the location of model sources, and [a] is the theoretical reduction-to-pole anomaly on that surface. The panel [c] is derived from the total-field magnetic anomaly mesh data shown in Figure 3 [A], at the altitudes of Figure 3 [B], and [e] is from the survey line data, Figure 3 [L], without grid interpolation. Panels [d] and [f] in Figure 4 are the results of conventional Fourier-method calculation with the assumption that the input data lie on a horizontal plane. Panel [d] is the result calculated from the gridded total-field anomaly Figure 3 [E], and [f] from Figure 3 [G] (reduced directly from the survey line data).

On panels [c] – [f], shaded areas show where the difference from the theoretical value [a] exceeds  $20\text{nT}$ . It is noted that these error zones spread more widely for results [d] and [f], probably because of the improper assumption that the magnetic anomaly is observed on a horizontal plane. Panel [c] shows calculated peak values that are smaller and contour lines that are distorted more than in panel [e], calculated by our proposed method. This demonstrates that our method of calculating the equivalent-source distribution directly from line data, and then rotating the directions of equivalent-source magnetisation and the ambient magnetic field, is the best method to recover reduction-to-pole anomalies.

## FIELD EXAMPLE

We applied the equivalent-source techniques above to an actual aeromagnetic survey in order to confirm their practicality with field data. In this survey area, a Tertiary volcanic complex with a cauldron structure is known from geological mapping. Three flights on the same day covered the survey area of approximately  $10\text{ km} \times 12\text{ km}$ , using a helicopter equipped with a nose-boom

cesium-vapour magnetometer sensor (Nakatsuka and Okuma, 2005). After removing the International Geomagnetic Reference Field (IGRF) (Nakatsuka, 2005) as a regional trend, and the diurnal variation of the magnetic field using data from a ground base station, we applied a passive magnetic compensation for the aircraft's magnetic field (Nakatsuka and Okuma, 2005) using data from a compensation test flight on the previous day.

To construct a total-field magnetic anomaly map, we applied two reduction procedures, one by way of gridded data and the other directly from survey line data, both with a surrounding zone of equivalent sources, and the results are shown in Figure 5 (A) and (B), respectively. The reduction surface (altitude), shown in Figure 6 (A), was smoothly averaged from actual flight altitude data. There is little difference between the results of the two procedures, probably because of the relatively high amplitudes of the large-scale magnetic anomalies. Although we cannot identify a “correct” solution in the field data, there is no indication of defects in either result. As was suggested in an earlier section, the shorter-wavelength anomalies are recovered more correctly by the method direct from line data, so it will be likely that the procedure of direct reduction from line data will produce a more realistic result.

The same data (survey line data) were also used to calculate the reduction-to-pole magnetic anomalies, by the method of rotating the equivalent-source magnetisation. The directions of magnetisation and ambient magnetic field are both assumed to be  $49^\circ\text{N}$  inclination,  $7^\circ\text{W}$  declination, calculated from the IGRF in the area. Figure 6 (B) is the result. The bipolar pattern of total-field anomalies seen in Figure 5 (A) and (B) has been converted successfully to a unipolar pattern, which represented clearly the cauldron structure and the distribution of other magnetic rock bodies.

## CONCLUDING REMARKS

In processing data from helicopter-borne aeromagnetic surveys

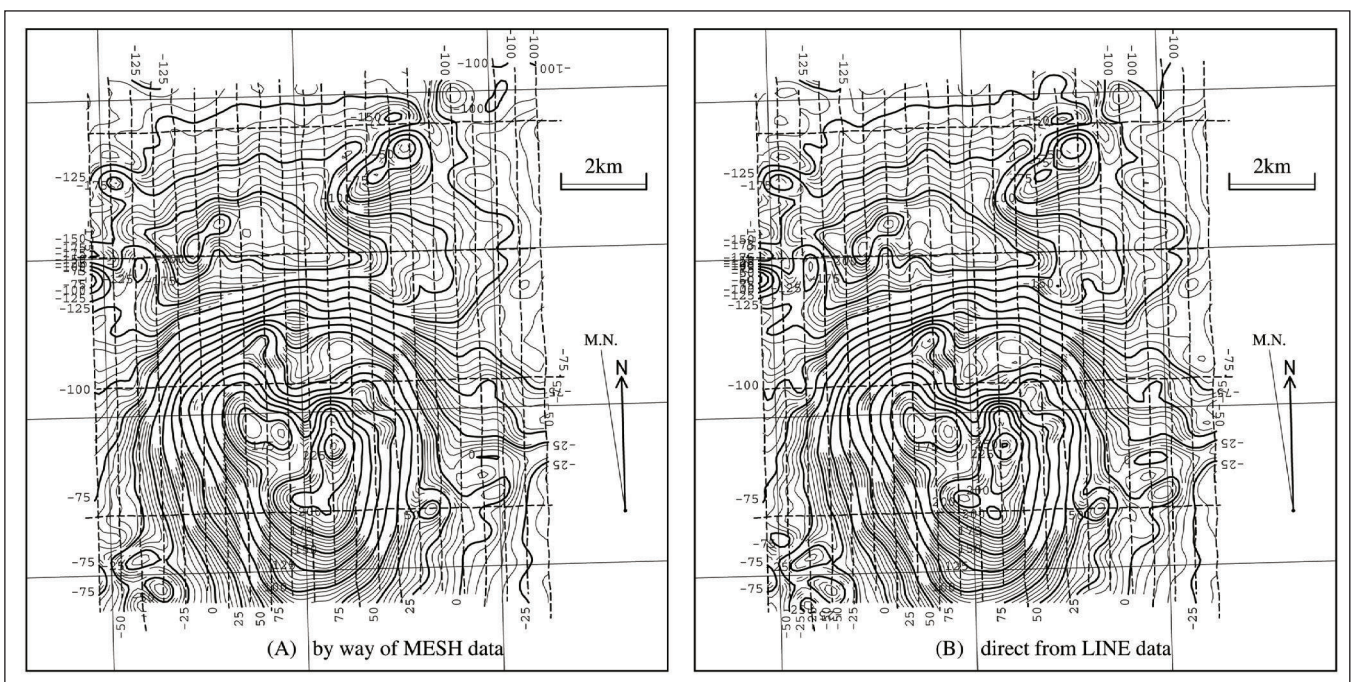


Fig. 5. Results of reduction of actual total-field survey data, by way of gridded data, and direct from survey line data. The contour interval is  $5\text{nT}$ , and dashed lines indicate the survey flight tracks. The reduction surface altitude is shown in Figure 6 (A).

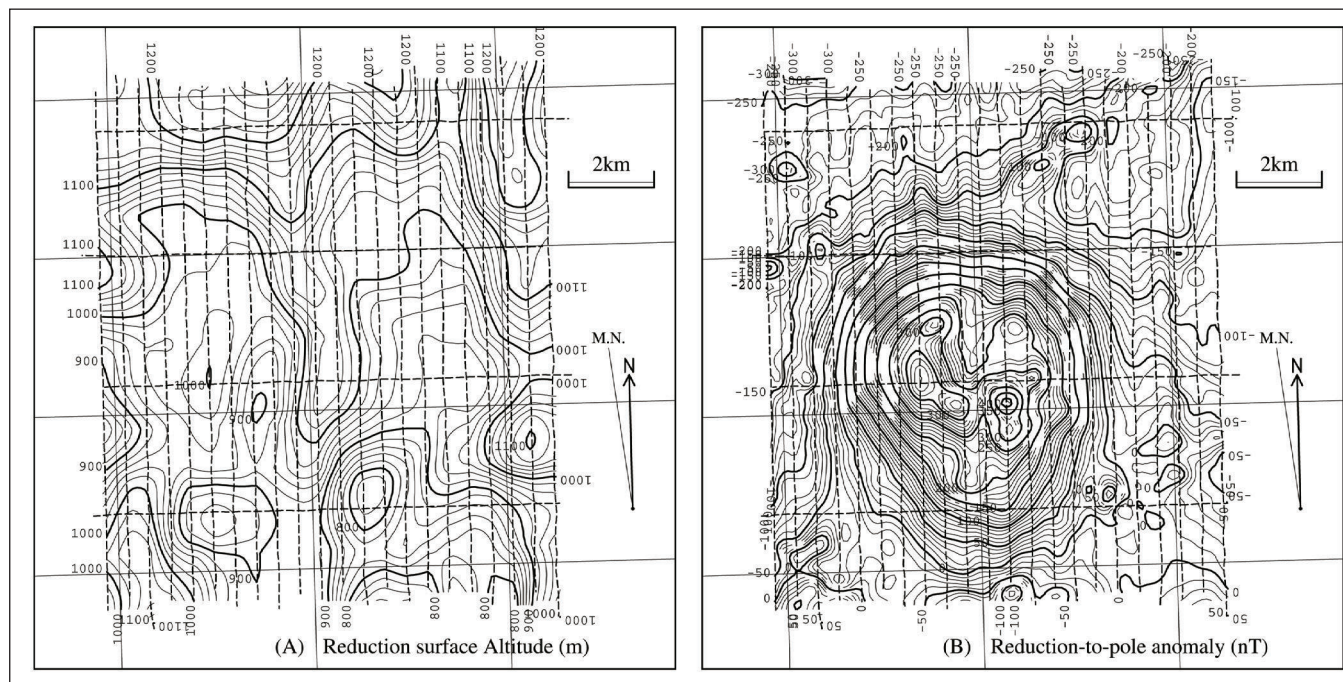


Fig. 6. Reduction surface altitude (A: 20m contour interval) and reduction-to-pole anomaly (B: 10nT contour interval) derived from actual survey data. The reduction surface is a smoothed version of the actual survey flight elevations. The reduction-to-pole anomaly (B) was extracted by the method of rotating equivalent-source magnetisation.

in mountainous regions, the reduction of data observed at varying elevations is a crucial problem. We have developed a method, and the appropriate software, to deal with such data using an equivalent-source technique based on properties of potential fields, and we have applied the method to synthetic models to examine its performance.

From the model studies, we make the following suggestions:

(1) The introduction of an additional zone of equivalent sources around the area of observation is useful to avoid edge effects in the calculated fields.

(2) When deriving equivalent sources from observed magnetic anomalies, the use of an intermediate step of grid interpolation by conventional methods may be detrimental, especially when observation altitudes are highly variable. Using our procedure of reduction using sources calculated directly from survey line data is recommended.

(3) Reduction-to-pole anomalies can be calculated efficiently at the same time as the altitude reduction, by using an equivalent-source model that includes magnetisation direction parameters, and rotating the directions of magnetisation and ambient magnetic field to the vertical for the final forward calculation.

(4) Although these reduction procedures include an inversion step that is usually an underdetermined problem, finding the minimum Euclidean norm solution using the conjugate gradient method gives an appropriate result.

The equivalent-source technique above was also applied to data from an actual survey, confirming that the method is practical.

This technique does not require extensive computing resources. The turn-around time for each processing workflow in this study was roughly several minutes, using a Linux OS on a 1 GHz Pentium III processor with 512 MB RAM.

## REFERENCES

- Briggs, I.C., 1974, Machine contouring using minimum curvature: *Geophysics*, **39**, 39–48.
- Cordell, L., 1992, A scattered equivalent-source method for interpolation and gridding of potential-field data in three dimensions: *Geophysics*, **57**, 629–636.
- Dampney, C.N.G., 1969, The equivalent source technique: *Geophysics*, **34**, 39–53.
- Hansen, R.O., and Miyazaki, Y., 1984, Continuation of potential fields between arbitrary surfaces: *Geophysics*, **49**, 787–795.
- Makino, M., Nakatsuka, T., Morijiri, R., Okubo, Y., Okuma, S., and Honkura, Y., 1993, Derivation of three-dimensional distribution of geomagnetic anomalies from magnetic values at various elevations: *Proceedings of the 88<sup>th</sup> SEGJ Conference*, 502–507.
- Nakatsuka, T., 1981, Reduction of magnetic anomalies to and from an arbitrary surface: *Butsuri-Tanko (Geophysical Exploration)*, **34**, 332–340.
- Nakatsuka, T., 1995, Minimum norm inversion of magnetic anomalies with application to aeromagnetic data in the Tanna area, Central Japan: *Journal of Geomagnetism and Geoelectricity*, **47**, 295–311.
- Nakatsuka, T., 2005, Calculation of the International Geomagnetic Reference Field (4): *Geological Survey of Japan Open-File Report no. 423*, 39pp.+Diskette. [Web Document]: Accessed 20 October, 2005. Available at <<http://www.gsj.jp/GDB/openfile/files/no0423/index.html>>.
- Nakatsuka, T., and Okuma, S., 2005, Development of helicopter-borne magnetic survey system in use of a nose boom magnetic sensor and its passive compensation for aircraft's magnetic field: *Butsuri Tansa (Geophysical Exploration)*, **58**, 421–429.
- Smith, W.H.F., and Wessel, P., 1990, Gridding with continuous curvature splines in tension: *Geophysics*, **55**, 293–305.
- Wessel, P., and Smith, W.H.F., 1998, New improved version of the Generic Mapping Tools released: *EOS, Transactions of the American Geophysical Union*, **79**, 579.

## ヘリコプター磁気探査データの高度リダクション処理

中塚 正<sup>1</sup>・大熊茂雄<sup>1</sup>

**要 旨：** 山岳地のヘリコプター磁気探査の場合には、高度変化に富む観測データの処理が重要であり、ヘリコプター磁気探査で普通に起こりうる3次元ランダム点での測定に対応したデータ処理ソフトウェアを開発した。等価ソース・等価アノマリを利用した任意曲面間のデータリダクション手法についてモデルスタディによる検討を行い、以下の結果を得た。(1) データ処理範囲の外側にも等価ソースの存在を仮定することにより、エッジ効果の軽減が図れる。(2) 観測データから等価ソースを導く上で、格子データへの補間を行うことは時に有害であり、測線データから等価ソースを直接導くのがよい。(3) 極磁力分布は、磁化方向を考慮した等価ソースの磁化方向の回転で計算できる。(4) 逆解析での不定解の問題は、共役勾配法によるノルム最小解で妥当な結果が得られる。また、実調査飛行例のデータに対して、測線データから等価ソースを直接導く方法と、さらに等価ソースの磁化方向の回転で極磁力分布を求める方法を適用し、妥当な結果の得られることを確認した。

**キーワード：** 磁気探査、リダクション、等価ソース、ノルム最小解、共役勾配法

## 고도가 변화하는 헬리콥터 탐사에서 얻어지는 자력이상의 변환

Tadashi Nakatsuka<sup>1</sup> and Shigeo Okuma<sup>1</sup>

**요 약：** 헬리콥터를 이용한 항공자력탐사는 정해진 고도를 따라 지표면에 평행하게 이루어지지만, 고해상도 탐사에서는 특히 측정이 이루어지는 고도가 너무 변화하여 평탄면으로 간주할 수 없는 경우가 있다. 이 연구에서는 모서리 효과를 조절할 수 있도록 주변 자력원이 포함되는 등가원 방법을 이용하여 이러한 자료를 변환하는 방법을 개발하였고, 3 차원적으로 무작위하게 분포하는 점의 자료를 직접적으로 모델화하였다. 이 문제는 일반적으로 under-determined 이지만 CG 법은 최소 norm 해를 찾을 수 있으며, 자력이상을 자력원과 연관시키는 조화함수를 선택할 자유가 있는데, 상향연속 함수 연산자가 선택되면 등가원 자체가 자력이상이 된다. 기본자기장의 방향으로의 자기 쌍극자 분포를 자력원으로 선택하면, 자기 쌍극자의 방향을 수직으로 돌려줌으로써 쉽게 자극화 변환 이상을 유도할 수 있다.

**주요어：** 자력탐사, 변환, 등가원, 절단오차, 최소 norm, CG

<sup>1</sup> 産業技術総合研究所 地質情報研究部門  
〒305-8567 茨城県つくば市東 1-1-1 中央第 7

<sup>1</sup> 산업기술종합연구소 지질정보연구부문